# Light-assisted spontaneous birefringence and magnetic-domain formation in a suspension of gyrotropic nanoparticles

Alexander A. Zharov and Alexander A. Zharov Jr.*
*Institute for Physics of Microstructures, Russian Academy of Sciences, Nizhny Novgorod 603950, Russia*

Nina A. Zharova
*Institute of Applied Physics, Russian Academy of Sciences, Nizhny Novgorod 603950, Russia*

(Received 28 April 2018; published 2 July 2018)

We show that linearly polarized light in a suspension of gyrotropic nanoparticles can experience modulation instability, which leads to spatial separation of right- and left-circularly polarized waves. Such a separation preserves zero full angular momentum of the electromagnetic field; thus, the time-reversal symmetry is broken only locally. Eventually, this instability results in the formation of the lattice of spatial solitons with alternating right and left circular polarization. As magnetic moments of nanoparticles tend to reorient parallel to the wave vector in circularly polarized light, every spatial soliton captures a static magnetic field directed along or opposite to the wave vector depending on the direction of the field angular momentum; therefore, the soliton lattice altogether looks like an array of magnetic domains with antiferromagnetic ordering.

DOI: 10.1103/PhysRevA.98.013802

## I. INTRODUCTION

The interaction of light with metamaterials has been the subject of careful and comprehensive studies in recent decades. Metamaterials are composites artificially nanostructured on subwavelength levels, whose macroscopic electromagnetic properties may significantly differ from those of natural media. Moreover, the desired properties can be imparted to a metamaterial through the design of its structural elements (meta-atoms). Indeed, to date, various kinds of metamaterials exhibiting unusual properties in different frequency domains from microwaves up to optics have been obtained. One of the primary motivations for developing, designing, and manufacturing metamaterials is the control of electromagnetic radiation at micrometer and nanometer scales. In this context, one can mention linear and nonlinear tunable negative index metamaterials [1–13], plasmonic materials including arrays of plasmonic nanoparticles [14–24], artificial hyperbolic media [25–28], all-dielectric metamaterials [29–33], etc. All those metamaterials pave the way toward making tunable and reconfigurable fast-acting nanoscale optical devices such as superlenses [34–37], nanolasers [38–40], nanoantennas [41–44], and biosensors [45–48].

Somewhat apart are recently suggested liquid metamaterials [49,50], which are easily reconfigurable, capable of filling the volumes of almost arbitrary shapes, and highly tunable. However, they are characterized by relatively slow response. Specific liquid metamaterials called liquid metacrystals [51–54] are predicted to possess extremely strong nonlinear properties due to both resonant response and orientational type of nonlinearity, which are not related to the nonlinearity of the substances comprising metamaterial [55].

Composites with inherent magnetic properties have certain advantages over nonmagnetic metamaterials. Chiral and gyrotropic media possess so-called optical activity that manifests itself as circular birefringence, leading to polarization rotation and circular dichroism. This, in turn, leads to a number of important magneto-optical effects, such as Faraday rotation of the polarization plane [56], and magneto-optical Kerr and Cotton-Mutton (or Voigt) effects [57]. These effects expand the possibilities of metamaterial applications. For instance, the magneto-optical Kerr effect can be prominently enhanced in nanostructured ferromagnetic metamaterials because of plasmon dipole resonance of individual pellets making up the composite [58]. Also, an electromagnetic analog of an electric diode [59] and nonlinear optical activity in metamaterials [60] have been demonstrated experimentally with metamaterials based on an array of nonlinear chiral meta-atoms.

In this paper, we report a class of nonlinear magneto-optical effects inherent in liquid optical metamaterials with gyrotropic nanoinclusions. These effects are caused by modulation instability of linearly polarized light, which results in spatial fragmentation of the initial beam into domains with right and left circular polarization.

In this context, it is relevant to mention that we consider nanoparticles in which the magnetization direction is frozen within the particle and the magnetic moment reorientation is due to the mechanical rotation of the particle with respect to the carrier liquid. This so-called Brownian mechanism of magnetic moment relaxation is different from Neel relaxation taking place in single-domain nanoparticles (usually, with diameter $\sim$ 5–10 nm and less), in which the magnetization can change its direction without mechanical rotation of the nanoparticle [61,76].

*Alexander.Zharov@gmail.com

 

## II. LIGHT-DRIVEN GYROTROPY

We consider the interaction of an optical frequency electromagnetic wave with a liquid metamaterial consisting of spherical magnetized ferromagnetic nanoparticles suspended in viscous liquid. It is well known that the gyrotropy of ferromagnetics in optics arises from the so-called gyroelectric effect [62] caused by spin-orbit interaction, which contributes only to the components of the dielectric tensor, while the magnetic permeability remains the unit tensor [63]. In Cartesian coordinates with the $z$ axis along the magnetization direction, the dielectric permittivity tensor of ferromagnetic material can be written as

$$\hat{\varepsilon} = \begin{pmatrix} \varepsilon_\perp & ig & 0 \\ -ig & \varepsilon_\perp & 0 \\ 0 & 0 & \varepsilon_\parallel \end{pmatrix}, \tag{1}$$

where $\varepsilon_\perp$ and $\varepsilon_\parallel$ are the transverse and longitudinal permittivity components, $g$ is the gyrotropy factor [hereinafter we assume a quasimonochromatic process: $\mathbf{E},\mathbf{H} \sim \exp(i\omega t)$]. The off-diagonal component of the dielectric tensor can be expressed with the help of the magneto-optical material constant $Q$, the so-called Voigt constant: $g = Q\varepsilon_\perp$ [64].

Bear in mind that usually $g \ll 1$ and $\varepsilon_\perp$ contains gyrotropy terms only $\sim g^2$, whereas $\varepsilon_\parallel$ does not depend on $g$; further we do not distinguish between $\varepsilon_\perp$ and $\varepsilon_\parallel$, assuming $\varepsilon_\perp = \varepsilon_\parallel = \varepsilon_p$. Consequently, the polarizability tensor of an individual ferromagnetic spherical meta-atom in the chosen Cartesian coordinate system takes the form

$$\hat{\alpha} = \begin{pmatrix} \alpha & iu\cos\theta & -iu\sin\phi\sin\theta \\ -iu\cos\theta & \alpha & iu\cos\phi\sin\theta \\ iu\sin\phi\sin\theta & -iu\cos\phi\sin\theta & \alpha \end{pmatrix}, \tag{2}$$

where $\alpha = a^3(\varepsilon_p - \varepsilon_l)/(\varepsilon_p + 2\varepsilon_l), u = 3g\varepsilon_l a^3/(\varepsilon_p + 2\varepsilon_l)^2, a$ is the radius of meta-atoms, $\varepsilon_l$ is the permittivity of the surrounding liquid, and $\phi$ and $\theta$ are the spherical angles defining the magnetization direction of an individual meta-atom.

As the meta-atoms are immersed into a liquid, they undergo Brownian motion due to thermal fluctuations. In turn, Brownian motion disorients the meta-atoms, which obviously changes the optical properties of the liquid metamaterial. Brownian reorientation of the meta-atoms can be taken into account in the case of thermodynamic equilibrium. The angular distribution of magnetic moments of the meta-atoms obeys the Gibbs statistics with the distribution function [65]

$$f(\phi,\theta) = A_0 \exp(-W/k_B T), \tag{3}$$

where $A_0$ is a normalization factor, $T$ is the temperature, $k_B$ is the Boltzmann constant, and the energy $W$ is given by

$$W = -\langle \mathbf{pE} + \mathbf{mH} - W_{\text{int}} \rangle \tag{4}$$

and is averaged over the period of the electromagnetic field. Here $\mathbf{p}$, $\mathbf{m}$ are the electric and magnetic moments of the meta-atom in an external electromagnetic field [66], angular brackets denote the averaging, and $W_{\text{int}}$ is the energy of interaction between neighboring meta-atoms. To estimate the interaction energy $W_{\text{int}}$ one can use the so-called Lorentz-Lorenz approach, which gives the relation between local and macroscopic electromagnetic fields [67] and takes into account the influence of environmental meta-atoms. To simplify the calculations, we assume that local and macroscopic fields are equal, which is correct for a rare enough colloid. Then, $W_{\text{int}}$ is negligibly small in comparison to the dipole energy.

It should be noted that our model is inapplicable below the critical temperature when the magnetic particles in the liquid metamaterial arrange in the domain structure because of magnetic dipole-dipole interaction. We consider the case when the thermal energy is greater than the magnetic dipole-dipole interaction energy, $k_b t \gg W_{\text{dd}}^{(m)}$, and this condition is satisfied for the estimation parameters used below.

The averaged electric dipole energy is

$$W = -\langle \mathbf{pE} \rangle = -\tfrac{1}{2}(\mathbf{pE}^* + \text{c.c.}), \tag{5}$$

where $\mathbf{p} = \hat{\alpha}\mathbf{E}$, c.c. means "complex conjugate," $(\dots)^* = \text{c.c.}$ The averaged energy of the magnetic dipole in Eq. (4) is zero in the case of a zero static external magnetic field. By substituting $\mathbf{p}$ into Eq. (5), we come to the explicit expression for the time-averaged dipole energy

$$\begin{aligned} W &= -I\text{Re}(\alpha) - i\text{Re}(u)(\mathbf{r}_0 \cdot [\mathbf{E}^* \times \mathbf{E}]) \\ &= -I\text{Re}(\alpha) - i\text{Re}(u) \\ &\quad \times (S_{xy}\cos\theta - S_{xz}\sin\phi\sin\theta + S_{yz}\cos\phi\sin\theta). \end{aligned} \tag{6}$$

Here $I = |\mathbf{E}|^2$, $S_{ik} = E_i^* E_k - E_i E_k^*$, and $\mathbf{r}_0 = (\cos\phi\sin\theta, \sin\phi\sin\theta, \cos\theta)$ is the unit vector. We assume that the distribution function is normalized as follows:

$$\int_0^{2\pi} d\phi \int_0^{\pi} f(\phi,\theta)\sin\theta d\theta = 1. \tag{7}$$

Let us consider transverse electromagnetic waves propagating in the $z$ direction. Such waves have two components of electric field, $E_x$ and $E_y$. Hence, the integral (7) contains only the term with $S_{xy}$ and can be calculated explicitly as

$$\begin{aligned} &Ae^{I\text{Re}\alpha/k_B T} \int_0^{2\pi} d\phi \int_0^{\pi} e^{i\text{Re}(u)S_{xy}\cos\theta/k_B T}\sin\theta \; d\theta \\ &= 4\pi A e^{I\text{Re}\alpha/k_B T}\frac{\sinh G}{G}, \end{aligned} \tag{8}$$

where $G = i\text{Re}(u)S_{xy}/k_B T$ is real valued. The normalization condition (7), together with Eq. (8) give the constant $A$:

$$A = \frac{G}{4\pi\sinh G}\exp(-I\text{Re}\alpha/k_B T). \tag{9}$$

To find the macroscopic polarizability $\bar{\alpha}_{ik}$ (or any other macroscopic physical parameter of the system) in thermal equilibrium one needs to average the microscopic $\alpha_{ik}$ with the distribution function

$$\bar{\alpha}_{ik} = \int_0^{2\pi} d\phi \int_0^{\pi} \alpha_{ik} f(\phi,\theta)\sin\theta \; d\theta. \tag{10}$$

Following this procedure, we find the components of the polarizability

$$\bar{\alpha}_{ii} = \alpha, \bar{\alpha}_{xy}^{\text{NL}} = -\bar{\alpha}_{yx}^{\text{NL}} = iuL(G) \tag{11}$$

and dielectric tensor

$$\varepsilon_{ik} = \varepsilon_l + 4\pi N\bar{\alpha}_{ik}, \tag{12}$$

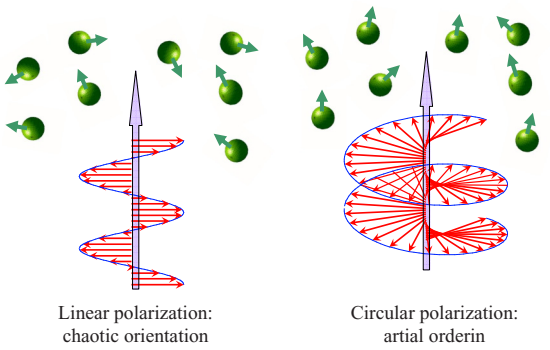


FIG. 1. Reorientation of magnetic nanoparticles in electromagnetic field: Left panel: linearly polarized light; magnetic moments are chaotically directed. Right panel: circularly polarized light; magnetic moments reorient along the light angular momentum.

where $N$ is the concentration of meta-atoms and $L$ is the so-called Langevin function [68]

$$L(G) = \frac{G - \tanh G}{G \tanh G}. \tag{13}$$

Thus, we have shown that a suspension of ferromagnetic nanoparticles behaves as a specific nonlinear medium with its nonlinear response leading to the light-driven gyrotropy. This is somehow related to the so-called hidden anisotropy (or gyrotropy), i.e., anisotropy at the microscopic level [69]. It appears as an emergence of imaginary off-diagonal terms in the macroscopic polarizability (and also permittivity) tensor, which are eventually responsible for birefringence and optical activity in the light field with nonzero angular momentum. The physical reason for this phenomenon is the reorientation of meta-atom magnetic moments toward the angular momentum of the electromagnetic field. It is schematically illustrated in Fig. 1 where the reorientation of the meta-atoms in the light wave with finite angular momentum is shown.

Such reorientation leads also to the emergence of macroscopic static magnetic field $B$, and this effect can be identified with the well-known inverse Faraday effect [70,71]. One should also note that the light-driven gyrotropy saturates, $\bar{\alpha}_{xy}, \bar{\alpha}_{yx} \to$ const, and $B \to B_{\max}$ [see Eq. (13)], in extremely intense light (or when $T \to 0$), when all the meta-atom magnetic moments orient strictly along the field angular momentum. Below, we consider some nonlinear magneto-optical effects caused by induced gyrotropy in colloids of ferromagnetic nanoparticles.

## III. MODULATION INSTABILITY OF LINEARLY POLARIZED LIGHT

Let us consider the propagation of a plane wave along the $z$ axis in a nonlinear medium with the dielectric tensor and polarizability described by Eqs. (11)–(13). In this case $E_x$ and $E_y$ components of the electric field obey the equations typically encountered in gyrotropic media:

$$\begin{aligned} d^2E_x/dz^2 + k_0^2\varepsilon E_x &= -ik_0^2\sigma^{\mathrm{NL}}E_y, \\ d^2E_y/dz^2 + k_0^2\varepsilon E_y &= ik_0^2\sigma^{\mathrm{NL}}E_x, \end{aligned} \tag{14}$$

where $\varepsilon = \varepsilon_l + 4\pi N\alpha$, $\sigma^{\mathrm{NL}} = 4\pi NuL(G)$, $G = \mathrm{Re}(u)(|E_R|^2 - |E_L|^2)/2k_BT$, $k_0 = \omega/c$, and $c$ is the speed of light. Assuming that $E_x, E_y \sim \exp(-ikz)$ we obtain the dispersion equation

$$k^2 = k_0^2\varepsilon \pm k_0^2\sigma^{\mathrm{NL}} \tag{15}$$

for two modes with right and left circular polarization, $E_{R,L} = E_x \pm iE_y$. With these new variables Eq. (14) becomes

$$\begin{aligned} d^2E_R/dz^2 + k_0^2\varepsilon E_R &= -k_0^2\sigma^{\mathrm{NL}}E_R, \\ d^2E_L/dz^2 + k_0^2\varepsilon E_L &= k_0^2\sigma^{\mathrm{NL}}E_L. \end{aligned} \tag{16}$$

In the realistic case $G \ll 1$ the function $L(G)$ can be represented as the first term of a Taylor expansion, $L(G) \approx G/3$ and, therefore, $\sigma^{\mathrm{NL}} \approx (2\pi N/3)u\mathrm{Re}(u)(|E_R|^2 - |E_L|^2)/2k_BT$. For the case of linearly polarized light $|E_R| = |E_L|$, $\sigma^{\mathrm{NL}} = 0$, and the set of equations (16) becomes degenerate. Both modes obey the same dispersion equation, which is quite obvious because the total angular momentum of light is zero in this case and magnetic moments of meta-atoms are disordered.

To simplify the analysis, one can take into account the small nonlinearity in Eq. (16) and apply the well-known approach of slowly varying amplitudes, looking for the solution of Eq. (16) in the form

$$E_{R,L} = A_{R,L}(z)\exp(-ik_0\sqrt{\varepsilon}z),$$

where $A_{R,L}$ are the slowly varying functions with respect to the phase factor. Substituting this expression into Eq. (16) and keeping only the first derivative, $dA_{R,L}/dz$, we find

$$\begin{aligned} 2ik_0\sqrt{\varepsilon}dA_R/dz &= k_0^2\sigma^{\mathrm{NL}}A_R, \\ 2ik_0\sqrt{\varepsilon}dA_L/dz &= -k_0^2\sigma^{\mathrm{NL}}A_L. \end{aligned} \tag{17}$$

The important question is: What happens to the linearly polarized electromagnetic wave when its amplitude is slightly perturbed? To address this stability problem it is necessary to allow for transverse dependence of the fields, $A_{R,L} = A_{R,L}(x,y,z)$. Strictly speaking, Eqs. (16) and (17) become incorrect in this case because of the appearance of the longitudinal ($E_z$) component of the electric field in the wave. Nevertheless, for "wide" beams, which can be described within the framework of a paraxial approximation [72], $E_z$ is negligibly small compared to $E_{x,y}$ ($|E_z| \ll |E_x|, |E_y|$), which allows us to consider the wave as quasitransversal. Then Eqs. (17) should be simply supplemented by transverse spatial Laplace operators, $\Delta_\perp = \partial^2/\partial x^2 + \partial^2/\partial y^2$:

$$\begin{aligned} 2ik_0\sqrt{\varepsilon}\partial A_R/\partial z - \Delta_\perp A_R &= k_0^2\sigma^{\mathrm{NL}}A_R, \\ 2ik_0\sqrt{\varepsilon}\partial A_L/\partial z - \Delta_\perp A_L &= -k_0^2\sigma^{\mathrm{NL}}A_L. \end{aligned} \tag{18}$$

It should be noted that in the absence of dissipation, these expressions conserve full angular momentum $S \sim \int_{-\infty}^{\infty}(|A_R|^2 - |A_L|^2)dxdy = $ const. Furthermore, the full energy flows in both right and left circularly polarized beams are conserved separately $P_{R,L} = \int_{-\infty}^{\infty}|A_{R,L}|^2dx\,dy = $ const.

To study the instability of linearly polarized light ($|A_R| = |A_L|$) we introduce the dimensionless variables

$$Z = \frac{z}{L_z}, \quad [X,Y] = \frac{[x,y]}{L_\perp}, \quad [U,V] = \frac{[A_R,A_L]}{A_C},$$

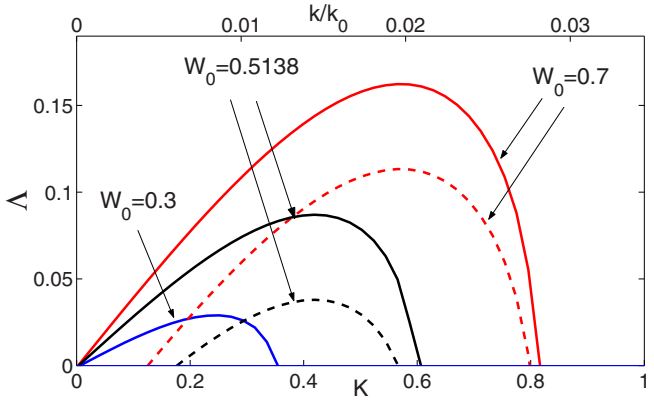


FIG. 2. Instability growth rate $\Lambda$ as a function of the transverse wave number $K_\perp$ for three amplitudes: $W_0 = 0.3$, 0.7, and 0.5138. The second wave-number scale given on the top is $k_\perp/k_0$. The dotted lines correspond to reduced growth rate in the case of nonzero damping ($\Lambda \to \Lambda - \gamma$ with $\gamma = 0.05$ and $W_0 = 0.5138, 0.7$), and in the case of $W_0 = 0.3$ the instability vanishes.

with

$$L_z = \frac{\sqrt{\varepsilon}}{k_0 4\pi u N}, \quad L_\perp = \frac{1}{k_0\sqrt{4\pi u N}}, \quad A_C = \sqrt{\frac{2k_B T}{\mathrm{Re}(u)}}, \tag{19}$$

and rewrite Eq. (18) as

$$2i\frac{\partial U}{\partial Z} - \frac{\partial^2 U}{\partial X^2} - \frac{\partial^2 U}{\partial Y^2} = L(|U|^2 - |V|^2)U,$$
$$2i\frac{\partial V}{\partial Z} - \frac{\partial^2 V}{\partial X^2} - \frac{\partial^2 V}{\partial Y^2} = -L(|U|^2 - |V|^2)V. \tag{20}$$

Then we perturb a given stationary solution $U = V = W_0$ [73] by a small ($|\delta_{R,L}| \ll W_0$) fluctuation, that is, $U = W_0 + \delta_R$ and $V = W_0 + \delta_L$. By linearizing Eq. (20) we obtain the following coupled equations for $\delta_R$, $\delta_L$:

$$2i\frac{\partial \delta_R}{\partial Z} - \frac{\partial^2 \delta_R}{\partial X^2} - \frac{\partial^2 \delta_R}{\partial Y^2} = \frac{W_0^2}{3}(\delta_R - \delta_L + \text{c.c.}),$$
$$2i\frac{\partial \delta_L}{\partial Z} - \frac{\partial^2 \delta_L}{\partial X^2} - \frac{\partial^2 \delta_L}{\partial Y^2} = -\frac{W_0^2}{3}(\delta_R - \delta_L + \text{c.c.}). \tag{21}$$

Now, setting $\delta_R, \delta_L \sim \exp(\Lambda Z - iK_X X - iK_Y Y)$ we find the dispersion equation

$$4\Lambda^2 = K_\perp^2(4W_0^2/3 - K_\perp^2), \quad K_\perp = \sqrt{K_X^2 + K_Y^2}. \tag{22}$$

The expression (22) describes a transversal modulation instability of linearly polarized light, which takes place at $0 < K_\perp < 2W_0/\sqrt{3}$, and the maximal growth rate is achieved for $K_\perp = W_0\sqrt{2/3}$. The dependence of the instability growth rate on the transverse wave number has the typical form that appears in the modulation instability described by the nonlinear Schrodinger equation. The presence of small energy losses leads to the appearance of a threshold of instability. Let $\gamma$ be the dimensionless coefficient of spatial damping of light in suspension, then the development of instability occurs only at $W_0 > W_C = \sqrt{3\gamma/2}$. The wave-number dependence of the instability growth rate is shown in Fig. 2 for three amplitudes: $W_0 = 0.3$, 0.7, and 0.5138, the last was used in numerical calculations (see below). Two wave-number scales (top and bottom) allows us to evaluate $\Lambda$ as a function of normalized $K_\perp$ and also of physical parameter $k_\perp/k_0$. The dotted lines correspond to the case of nonzero damping ($\Lambda \to \Lambda - \gamma$ with $\gamma = 0.05$). One can see the growth rate reduction for $W_0 = 0.5138$ and 0.7, but in the case of smallest $W_0$ the instability vanishes.

Such an instability means that the initial linearly polarized light beam splits into spatial domains of right and left circular polarization (with conservation of total zero angular momentum). Furthermore, orientational ordering of the magnetic moments within the domains of right or left circular polarization results in a generation of a static magnetic field, i.e., it gives rise to spontaneous local breaking of time-reversal symmetry. This effect of spatially separated spontaneous birefringence arising in suspension of gyrotropic nanoparticles has not been predicted so far.

To estimate the characteristic spatial and intensity scales, we use the following set of physical parameters: nanoparticle radius $a = 35$ nm; meta-atom concentration $N = 10^{15}$ cm$^{-3}$; permittivity of liquid (water) $\varepsilon_l = 1.77$; room temperature $T = 293$ K; operating wavelength $\lambda = 700$ nm; material of the meta-atom cobalt ferrite ($CoFe_2O_4$) with $\varepsilon_p = 7 - 0.5i$ and gyration $g = 0.04 - 0.02i$, such as the magneto-optical constant $Q \approx 6\times10^{-3}$ [74]. For these parameters the characteristic longitudinal and transverse scale-lengths are $L_z = 0.0128$ cm, $L_\perp = 3.2\times10^{-4}$ cm, and characteristic amplitude $A_C = 973$ esu.

## IV. SPATIAL SOLITONS AND MAGNETIC-DOMAIN FORMATION

In general case, the solutions of Eqs. (20) can be obtained only numerically. Nevertheless, preliminary theoretical analysis can reveal some important properties of nonlinear light-beam dynamics. It is important to notice that in the field of purely right or left circular polarization, Eqs. (20) describe light propagation in nonlinear Kerr-type medium with self-focusing nonlinearity. The admixture of opposite polarization plays the role of a defocusing medium inhomogeneity. Hence, when the field of opposite polarization is relatively weak, its effect can be overcome, and the self-focusing eventually leads to the formation of a self-consistent waveguide called "spatial soliton" (or "filament"), which captures the light with nonzero field angular momentum and does not experience diffraction spreading.

Filamentation of a linearly polarized wave generates spatial solitons in pairs, each one of the pair carrying opposite field angular momenta. In the framework of perturbation theory, the solitons with opposite polarization repel each other, and with the same polarization attract each other. This takes place in direct analogy with interaction of in-phase and out-of-phase spatial solitons in the medium with cubic Kerr-type nonlinearity [75]. Therefore, one can expect formation of a lattice of filaments with alternating right and left circular polarizations. Bearing in mind the generation of static magnetic field along the light angular momentum inside each filament, one can consider this phenomenon as a formation of magnetic domains with antiferromagnetic ordering.

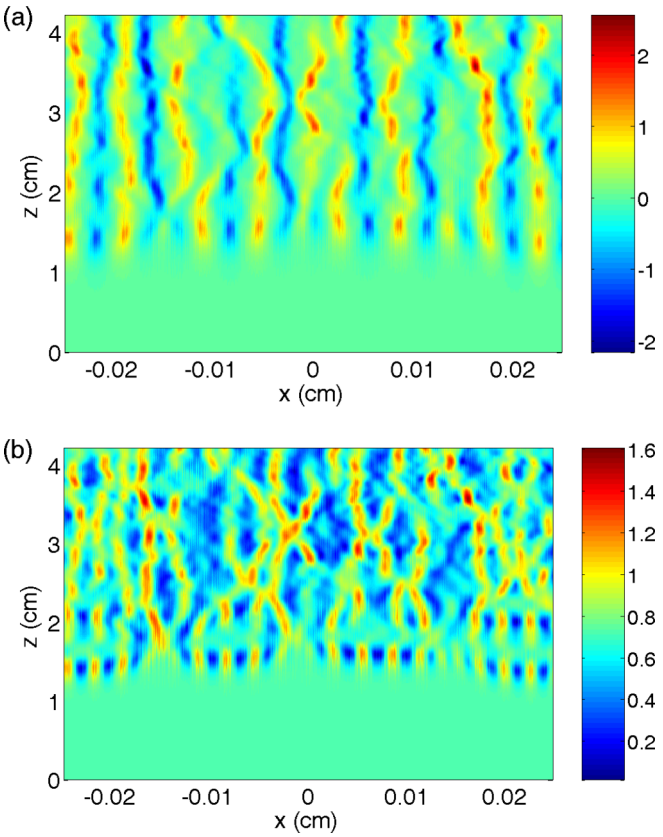


FIG. 3. Nonlinear spatial dynamics of (a) the helicity function $G(x,z) = |U|^2 - |V|^2$ and (b) the total field amplitude $\sqrt{|U|^2 + |V|^2}(x,z)$. Initial linearly polarized plane wave with the amplitude $\sqrt{2}W_0 = 0.73A_C$ perturbed by small random noise undergoes modulation instability and eventually splits into left and right polarized filaments.

The magnetic induction $B$ inside the filament can be estimated as

$$B \approx \frac{(4\pi)^2}{3} a^3 N M_R \rho,$$

where $\rho = 5.3\ \mathrm{g/cm^3}$ is the density and $M_R$ is the remanence of cobalt ferrite, which is about 30% of saturation magnetization, $M_R \approx 0.34 M_S \approx 13$ emu/g [76]. This estimation gives the maximum value of magnetic induction inside the filament, $B_{\max} \approx 150$ G, for the case of identically oriented magnetic moments of the meta-atoms. When the intensity of light is not sufficient fora saturation regime the magnitude of $B$ reduces to $B = B_{\max} L(G)$, where $L(G)$ is the Langevin function (13).

The validity of this simple qualitative analysis was confirmed by numerical solution of the full set of nonlinear equations (20), which provided the long-distance spatial dynamics of the light wave.

First, we have considered the (1+1)-dimensional problem and simulated the spatial evolution of a linearly polarized plane wave

$$U_0 = W_0(1 + r), \quad V_0 = W_0,$$

where $W_0 = 0.5138$ (the corresponding dimensional value is $\tilde{W}_0 = 500$ esu) and random perturbation $r$ is uniformly distributed on the interval $[-0.05, 0.05]$ with zero mean value.

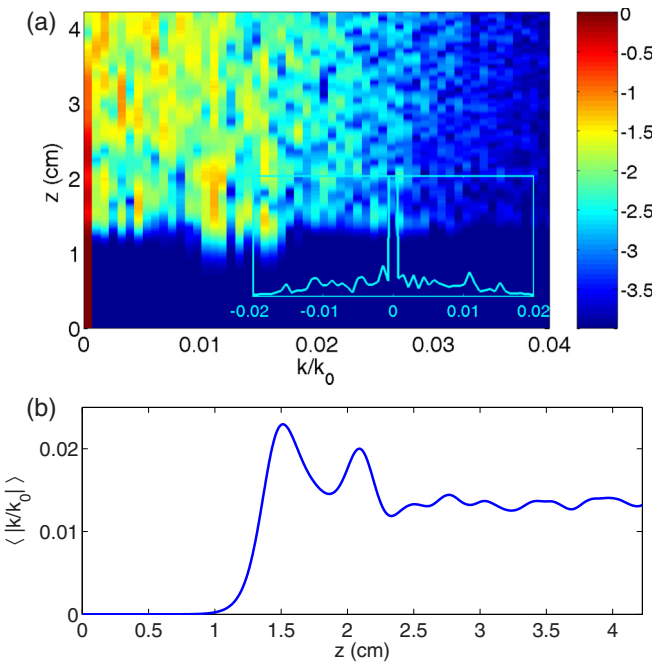


FIG. 4. (a) Spatial evolution of the field spectrum, $W_k = |U|_k^2 + |V|_k^2$ of initial linearly polarized plane wave. The color illustrates the function $\log_{10} W_k(k,z)$, and the spectrum averaged over the propagation distance, $\langle W_k \rangle (k/k_0)$ is shown in the inset. (b) Mean wave number of the field spectrum, $\langle k/k_0 \rangle = \int |k|/k_0 W_k dk / \int W_k dk$, as a function the propagation distance $z$.

The amplitude of the linearly polarized wave is $\sqrt{2}W_0 = 0.73$, which corresponds to the light intensity $6\times10^7\ \mathrm{W/cm^2}$. In simulations, we used periodic boundary conditions.

The local light helicity is characterized by the function $G = |U|^2 - |V|^2$, which enters as an argument of the function $L$ in Eqs. (20), and in the following we mostly use the function $G$ for the representation of numerical results.

Figure 3 shows spatial evolution of (a) the helicity function $G(x,z) = |U|^2 - |V|^2$ and (b) the total field amplitude $|E| = \sqrt{|U|^2 + |V|^2}(x,z)$. Initial noise evolves eventually into a set of filaments with the antiferromagnetic ordering. Wide-spectrum initial noise results in nonstable propagation with colliding and sometimes merging filaments; however, the width of the filaments is maintained more or less constant. One can also see breathing vibrations of the amplitude and the width of filaments. It should be noted that in the center of the filaments the functions $|G|$ and $|E|^2$ coincide closely, and thus light has nearly perfect right- or left-hand circular polarization.

The characteristic features of the spatial spectrum are shown in Fig. 4. The above estimations predict the maximum growth rate at $k_{\mathrm{opt}}/k_0 \approx 0.0145$ for our parameters and, indeed, the perturbation with this wave number grows faster than the other spectral noise components [see Fig. 4(a)]. The spectrum-averaged wave number $\langle k(z) \rangle = \int |k| W_k dk / \int W_k dk$ [Fig. 4(b)] initially strongly exceeds $k_{\mathrm{opt}}$. However, its value at the final (nonlinear) stage of instability approaches this optimal value. A pronounced oscillatory dependence of $\langle k \rangle$ on the propagation distance can also be seen in Fig. 4(b), and this is another manifestation of the breathing behavior of the filaments.

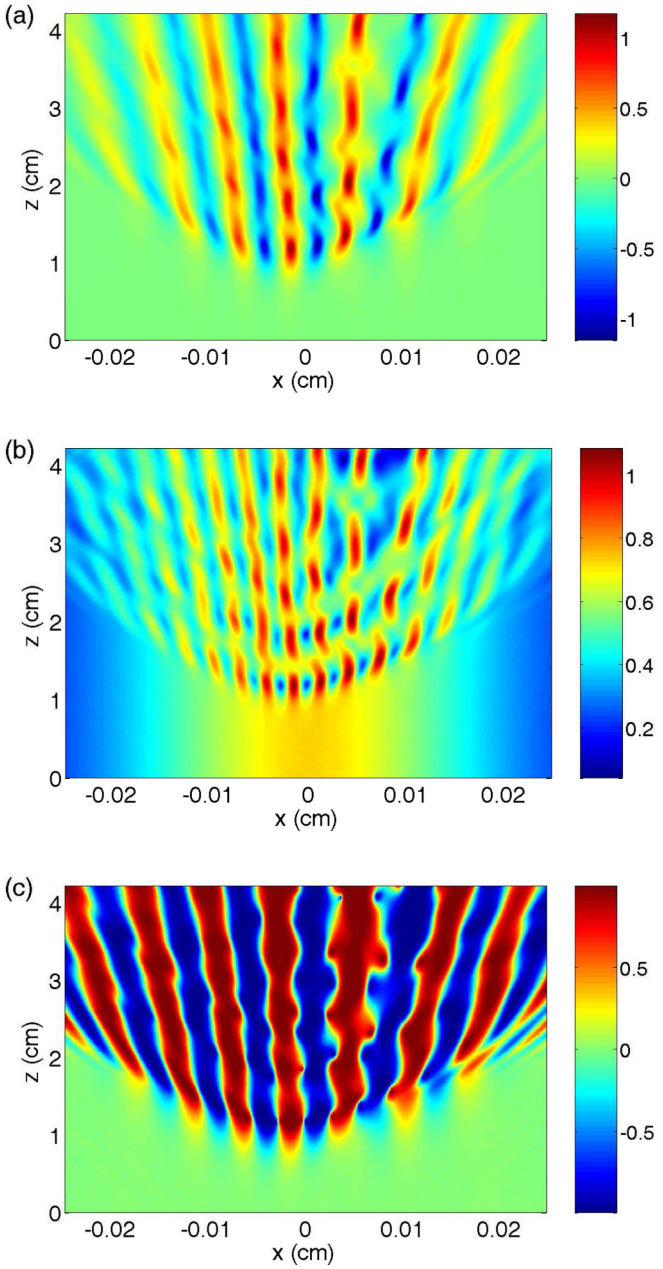


FIG. 5. Nonlinear spatial dynamics of (a) the helicity function $G(x,z) = |U|^2 - |V|^2$, (b) the total field amplitude $\sqrt{|U|^2 + |V|^2}(x,z)$, and (c) the normalized helicity density $C = (|U|^2 - |V|^2)/(|U|^2 + |V|^2)$. Initial linearly polarized bell-shaped beam with the amplitude $0.73A_C$ and the width 0.0144 cm perturbed by small random noise undergoes modulation instability and eventually splits into left and right polarized filaments. The other parameters of the simulation are given in the text.

Then, we have simulated the propagation of the linearly polarized light beam with the initial profile of the form

$$U_0 = \frac{W_0(1+r)}{\cosh(X/b_x)}, \quad V_0 = \frac{W_0}{\cosh(X/b_x)},$$

with the same amplitude $W_0 = 0.5138$ of the circularly polarized components and the width $b_x = 45$ (the corresponding dimensional width is $\tilde{b}_x = 0.0144\,\text{cm} = 208\lambda$). Here $r$ is again

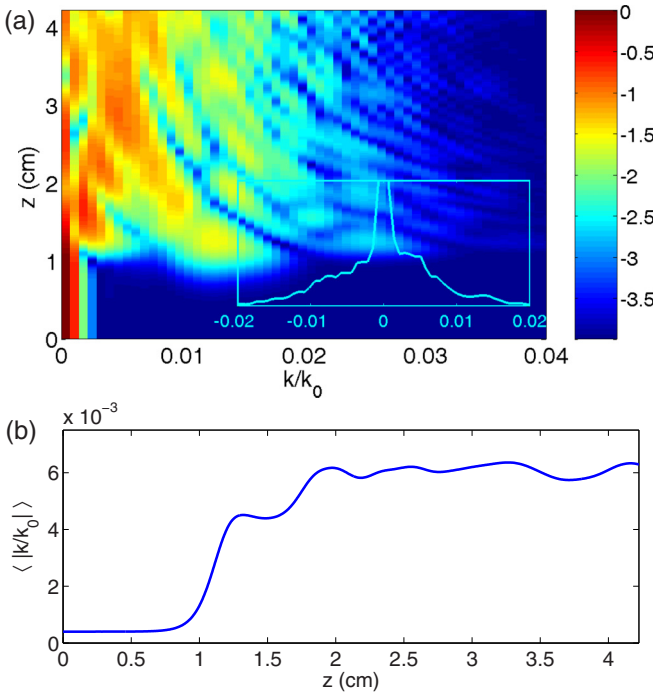


FIG. 6. (a) Spatial evolution of the field spectrum $W_k = |U|_k^2 + |V|_k^2$ of initial linearly polarized bell-shaped beam. The color illustrates the function $\log_{10} W_k(k,z)$, and the spectrum averaged over the propagation distance $\langle W_k \rangle_z$ as a function of $k/k_0$ is shown in the inset. (b) Mean wave number of the field spectrum $\bar{k}/k_0 = \int |k|/k_0 W_k dk / \int W_k dk$ as a function the propagation distance $z$.

a random perturbation uniformly distributed on the interval $[-0.05, 0.05]$ with zero mean value.

Figure 5 shows spatial evolution of (a) the helicity function $G(x,z) = |U|^2 - |V|^2$, (b) the total field amplitude $\sqrt{|U|^2 + |V|^2}(x,z)$, and (c) the normalized helicity density $C = (|U|^2 - |V|^2)/(|U|^2 + |V|^2)$ of the (1+1)-dimensional bell-shaped beam. Initial noise evolves into a set of filaments propagating at different angles with respect to the incident direction. The total width of the beam increases whereas the width of the filaments does not. It should be noted that the propagation of filaments is much more stable in this case, and the breathing vibrations are less pronounced. The normalized helicity density $C(x,z)$ gives a chiral portion of the total intensity and illustrates the "purity" of the light polarization, and one can see that its spatial dependence is very sharp, looking like a step function. Thus, the splitting of the beam into multiple filaments is distinct.

The spectral features are illustrated in Fig. 6. The mean wave number of the field spectrum, $\langle k \rangle = \int |k| W_k dk / \int W_k dk$ again oscillates and considerably differs from $k_{\text{opt}}$, though in this case it is less than the optimal value. This is obvious since the effective value of the initial field is noticeably less than its amplitude.

More interesting seems the two-dimensional problem where the medium nonlinearity can lead to the self-focusing of light with creation of highly localized hot spots, instead of quasistationary propagation of nonlinear filaments. However, the nonlinear dependence $L(G)$ saturates already for $G \sim 2$,

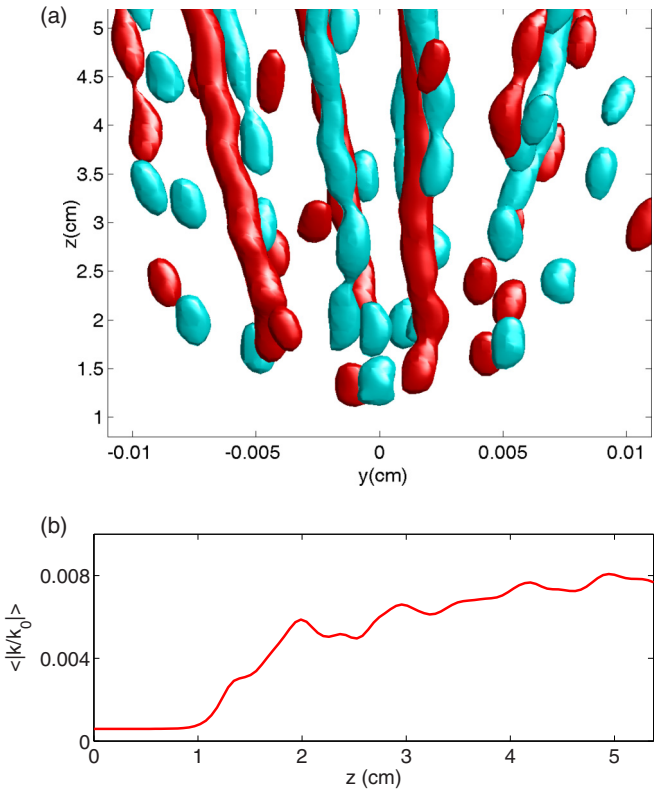


FIG. 7. (a) Nonlinear spatial dynamics of the helicity function $G(x,y,z) = |U|^2 - |V|^2$ of initial linearly polarized 2D wave beam: the isosurface $G(x,y,z) = 1.34$ (red filaments) and $G(x,y,z) = -1.34$ (blue filaments). (b) Mean wave number of the field spectrum $\langle k/k_0 \rangle = \int \sqrt{k_x^2 + k_y^2}/k_0 W_k dk / \int W_k dk$ as a function of the propagation distance $z$.

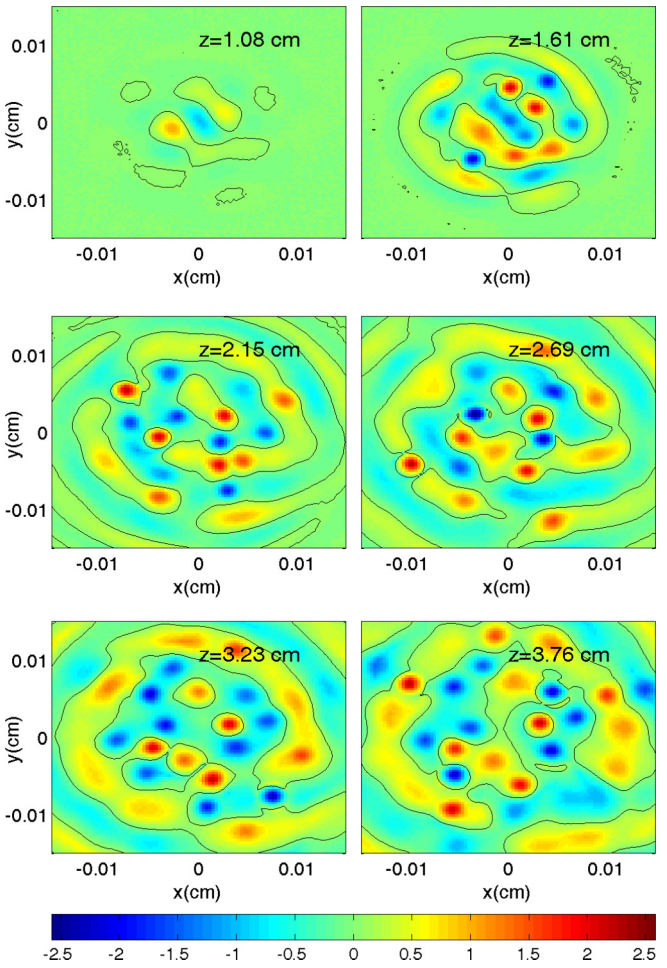


FIG. 8. Nonlinear spatial dynamics of initial linearly polarized 2D wave beam. The distribution of the function $F(x,y) = |U| - |V|$ is depicted at different $z$ positions. Black contour denotes points where $F = 0$, and thus the field is linearly polarized.

and this prevents strong focusing of light. The results of numerical simulation of the spatial evolution of the initial two-dimensional (2D) bell-shaped beam

$$U_0 = \frac{A_0(1+r)}{\cosh(\sqrt{X^2+Y^2}/b_\perp)},$$
$$V_0 = \frac{A_0}{\cosh(\sqrt{X^2+Y^2}/b_\perp)},$$

with the amplitude of circularly polarized components $A_0 = 0.5138$ and the width $b_\perp = 30$, and 2D uniform random perturbation $r$ ($r \in [-0.05, 0.05]$) are illustrated in Fig. 7.

Our numerical simulations show that the maximal value of helicity density is $|G|_{\max} = 6.7$, which coincides with the maximum of intensity, $\max(|U|^2 + |V|^2)$. Thus maximal field amplification compared to its original value is about 3.5. The nonlinearity saturation results in the similarity of the $z$ dependencies in transverse 2D and 1D field patterns, as seen in Fig. 7(a). It should be noted that the transverse characteristic scale (and the respective wave number) of the field pattern [see Fig. 7(b)] takes intermediate values between those in in Figs. 5 and 6. However, in both (1+1)D and (1+2)D cases the long-distance behavior is characterized by the concentration of right and left circularly polarized light in filaments.

For demonstration purposes, we also represent in Fig. 8 a set of field patterns where the function $F = |U| - |V|$ is shown in the $x$-$y$ plane taken at different $z$ positions. The black contour denotes points where the field has linear polarization.

## V. CONCLUSION

In conclusion, we have considered the interaction of light with suspension of spherical gyrotropic (ferromagnetic) nanoparticles. Within the kinetic approach, taking into account Brownian disordering of nanoparticles, we have obtained the nonlinear polarizability of this colloid and derived equations governing the propagation of light in such a liquid metamaterial. Our analytical and numerical study has shown that linearly polarized light undergoes a filamentation instability. As a result, the light beam with zero angular momentum splits into an array of spatial filaments with nonzero different-sign angular momenta. Moreover, every filament traps a constant magnetic field, thus the initially chaotic suspension changes into an ordered magnetic structure with antiferromagnetic ordering.

It should be noted that this effect does not set major limitations for the meta-atom size, identity, or frequency band (only allowing that light can propagate through colloid), and there is no need for extremely high intensity light. Therefore, we believe that the effect of spatial separation of different circular polarizations can find practical applications in optics.


## ACKNOWLEDGMENTS

We are thankful for the support from Russian Foundation for Basic Research through Grants No. 17-02-00281 and No. 16-02-00556. This work was also partially supported by FASO, Project No. 0035-2014-0201.



[1] D. R. Smith, W. J. Padilla, D. C. Vier, S. C. Nemat-Nasser, and S. Schultz, Phys. Rev. Lett. **84**, 4184 (2000).

[2] R. A. Shelby, D. R. Smith, and S. Schultz, Science **292**, 77 (2001).

[3] S. Linden, C. Enkrich, M. Wegener, T. Zhou, T. Kochny, and C. M. Soukoulis, Science **306**, 1351 (2004).

[4] S. Zhang, W. Fan, B. K. Minhas, A. Frauenglass, K. J. Malloy, and S. R. J. Brueck, Phys. Rev. Lett. **94**, 037402 (2005).

[5] G. Dolling, M. Wegener, C. M. Soukoulis, and S. Linden, Opt. Lett. **32**, 53 (2007).

[6] U. K. Chettiar, A. V. Kidishev, H. K. Yuan, W. Cai, S. Xiao, V. P. Drachev, and V. M. Shalaev, Opt. Lett. **32**, 1671 (2007).

[7] H. J. Lezec, J. A. Dionne, and H. A. Atwater, Science **316**, 430 (2007).

[8] A. Minovich, J. Farnell, D. N. Neshev, I. McKervacher, F. Karouta, J. Tian, D. A. Powell, I. V. Shadrivov, H. H. Tan, C. Jagadish, and Y. S. Kivshar, Appl. Phys. Lett. **100**, 121113 (2012).

[9] A. A. Zharov, I. V. Shadrivov, and Y. S. Kivshar, Phys. Rev. Lett. **91**, 037401 (2003).

[10] I. V. Shadrivov, A. A. Sukhorukov, Y. S. Kivshar, A. A. Zharov, A. D. Boardman, and P. Egan, Phys. Rev. E **69**, 016617 (2004).

[11] M. Lapine, I. V. Shadrivov, D. A. Powell, and Y. S. Kivshar, Nat. Mater. **11**, 30 (2012).

[12] M. Lapine, I. V. Shadrivov, D. A. Powell, and Y. S. Kivshar, Sci. Rep. **1**, 138 (2011).

[13] A. P. Slobozhanyuk, M. Lapine, D. A. Powell, I. V. Shadrivov, Y. S. Kivshar, R. C. McPherdan, and P. A. Belov, Adv. Mater. **25**, 3409 (2013).

[14] W. L. Barnes, A. Dereux, and A. Ebbensen, Nature **424**, 824 (2003).

[15] J. A. Fan, K. Bao, L. Sun, J. Bao, V. N. Manoharau, P. Nordlander, and F. Capasso, Nano Lett. **12**, 5318 (2012).

[16] A. Wiener, A. I. Fernandez-Dominquez, A. P. Horsfield, J. B. Pendry, and S. A. Maier, Nano Lett. **12**, 3308 (2012).

[17] A. Boltasseva and H. A. Atwater, Science **331**, 290 (2011).

[18] V. M. Shalaev and S. Kawata, *Nanophotonics with Surface Plasmons* (Elsevier Science, New York, 2007).

[19] A. A. Zharov and R. E. Noskov, Proc. SPIE **6581**, 658106 (2007).

[20] R. E. Noskov, A. A. Zharov, and M. V. Tsarev, Phys. Rev. B **82**, 073404 (2010).

[21] D. K. Gramotnev and S. I. Bozhevolnyi, Nat. Photon. **4**, 83 (2010).

[22] E. Wang, T. P. White, and K. R. Catchpole, Opt. Express **20**, 13226 (2012).

[23] J. B. Pendry, L. Martin-Moreno, and F. J. Garsia-Vidal, Science **305**, 847 (2004).

[24] J. T. Shen, P. B. Catrysse, and S. Fan, Phys. Rev. Lett. **94**, 197401 (2005).

[25] M. A. Noginov, Y. A. Barnakov, G. Zhu, T. Tumkur, H. Li, and E. E. Narimanov, Appl. Phys. Lett. **94**, 151105 (2009).

[26] Y. Guo, W. Newman, C. L. Cortes, and Z. Jacob, Adv. Opt. Electron. **2012**, 452502 (2012).

[27] A. Poddubny, I. V. Iorsh, P. A. Belov, and Y. S. Kivshar, Nat. Photon. **7**, 948 (2013).

[28] S. S. Kruk, Z. J. Wong, E. Pshenay-Severin, K. O'Brien, D. N. Neshev, Y. S. Kivshar, and X. Zhang, Nat. Commun. **7**, 11329 (2016).

[29] Q. Zhao, J. Zhou, F. Zhang, and D. Lippens, Mater. Today **12**, 60 (2009).

[30] X. Liu, K. Fan, I. V. Shadrivov, and W. J. Padilla, Opt. Express **25**, 191 (2017).

[31] M. A. Cole, D. A. Powell, and I. V. Shadrivov, Nanotechnology **27**, 424003 (2016).

[32] I. Staude, A. E. Miroshnichenko, M. Decker, N. T. Fofaug, S. Liu, E. Gonzales, J. Dominguez, T. S. Luk, D. N. Neshev, I. Brener, and Y. S. Kivshar, ACS Nano **7**, 7824 (2013).

[33] Y. Kivshar and A. Miroshnichenko, Opt. Photon. News **28**, 24 (2017).

[34] P. A. Belov, Y. Hao, and S. Sudhakaran, Phys. Rev. B **73**, 033108 (2006).

[35] M. G. Silveirinha, P. A. Belov, and C. R. Simovski, Phys. Rev. B **75**, 035108 (2007).

[36] A. A. Zharov, N. A. Zharova, and R. E. Noskov, JETP **109**, 734 (2009).

[37] S. Kawata, A. Ono, and P. Verma, Nat. Photon. **2**, 438 (2008).

[38] D. J. Bergman and M. I. Stockman, Phys. Rev. Lett. **90**, 027402 (2003).

[39] L. Cao and M. L. Brongersma, Nat. Photon. **3**, 12 (2009).

[40] X. Meng, A. V. Kidishev, K. Fujita, K. Tanaka, and V. M. Shalaev, Nano Lett. **13**, 4106 (2013).

[41] A. Alu and N. Engheta, Nat. Photon. **2**, 307 (2008).

[42] L. Novotny, Nature **455**, 887 (2008).

[43] L. Novotny and N. van Hulst, Nat. Photon. **5**, 83 (2011).

[44] S. Kruk, B. Hopkins, I. I. Kravchenko, A. Miroshnichenko, D. N. Neshev, and Y. S. Kivshar, APL Photon. **1**, 030801 (2016).

[45] J. N. Anker, W. P. Hall, O. Lyandres, N. C. Shah, J. Zhao, and R. P. van Duyne, Nat. Mater. **7**, 442 (2008).

[46] K. A. Willets and R. P. van Duyne, Annu. Rev. Phys. Chem. **58**, 267 (2007).

[47] N. T. R. N. Kumara, Y. F. C. Chau, J.-W. Huang, H. J. Huang, C.-T. Lin, and H.-P. Chiang, J. Opt. **18**, 115003 (2016).

[48] Y. F. C. Chau, J.-Y. Syu, C.-T. Chao, H.-P. Chiang, and C. M. Lim, J. Phys. D: Appl. Phys. **50**, 045105 (2017).

[49] Y. A. Urzhumov, G. Shvets, J. A. Fan, F. Capasso, D. Brandl, and P. Nordlander, Opt. Express **15**, 14129 (2007).

[50] M. Fruhnert, S. Muhlig, F. Lederer, and C. Rockstuhl, Phys. Rev. B **89**, 075408 (2014).
[51] A. A. Zharov, A. A. Zharov, Jr., and N. A. Zharova, J. Opt. Soc. Am. B **31**, 559 (2014).
[52] A. A. Zharov, A. A. Zharov, Jr., and N. A. Zharova, Phys. Rev. E **90**, 023207 (2014).
[53] N. A. Zharova, A. A. Zharov, and A. A. Zharov, Jr., J. Opt. Soc. Am. B **33**, 594 (2016).
[54] A. A. Zharov Jr., N. A. Zharova, and A. A. Zharov, J. Opt. Soc. Am. B **34**, 546 (2017).
[55] M. Liu, K. Fan, W. Padilla, X. Zhang, and I. V. Shadrivov, Adv. Mater. **28**, 1553 (2016).
[56] F. A. Jenkins and H. E. White, *Fundamentals of Optics*, 4th ed. (McGraw-Hill, New York, 1976).
[57] A. K. Zvezdin and V. A. Kotov, *Modern Magnetooptics and Magnetooptical Materials* (IOP Publishing, Bristol, UK, 1997).
[58] A. A. Zharov and V. V. Kurin, J. Appl. Phys. **102**, 123514 (2007).
[59] I. V. Shadrivov, V. A. Fedotov, D. A. Powell, Y. S. Kivshar, and N. I. Zheludev, New J. Phys. **13**, 033025 (2011).
[60] I. V. Shadrivov, Appl. Phys. Lett. **101**, 041911 (2012).
[61] L. Vekas, Adv. Sci. Tech. **54**, 127 (2008).
[62] H. J. Zeiger and G. W. Pratt, *Magnetic Interaction in Solids* (Oxford University Press, Oxford, 1973).
[63] L. D. Landau and E. M. Lifshitz, *Quantum Mechanics: Non-Relativistic Theory*, 3rd ed. (Pergamon Press, New York, 1977).
[64] J. Zak, E. R. Moog, C. Liu, and S. D. Bader, Phys. Rev. B **43**, 6423 (1991).
[65] L. D. Landau and E. M. Lifshitz, *Statistical Physics*, 3rd ed. (Butterworth-Heinemann, Boston, 1980).
[66] L. D. Landau and E. M. Lifshitz, *The Classical Theory of Field*, 4th ed. (Butterworth-Heinemann, Boston, 1975).
[67] M. Born and E. Wolf, *Principles of Optics: Theory of Propagation, Interference and Diffraction of Light*, 7th ed. (Cambridge University Press, Cambridge, England, 2002).
[68] C. Kittel, *Introduction to Solid State Physics*, 8th ed. (Wiley, New York, 2005).
[69] V. L. Erukhimov and V. E. Semenov, Radiophys. Quantum Electron. **41**, 571 (1998).
[70] J. Deschamps, M. Fitaire, and M. Lagoutte, Phys. Rev. Lett. **25**, 1330 (1970).
[71] R. Hertel, J. Magn. Magn. Mater. **303**, L1 (2006).
[72] M. V. Vinogradova, O. V. Rudenko, and A. P. Sukhorukov, *The Wave Theory* (Nauka, Moscow, 1990).
[73] Without loss of generality, $W_0$ is considered as a real value.
[74] C. Himcinschi, I. Vrejoiu, G. Salvan, M. Fronk, A. Talkenberger, D. R. T. Zahn, D. Rafaja, and J. Kortus, J. Appl. Phys. **113**, 084101 (2013).
[75] G. I. Stegeman and M. Segev, Science **286**, 1518 (1999).
[76] S. Berkum, J. T. Dee, A. P. Philipse, and B. H. Erne, Int. J. Mol. Sci. **14**, 10162 (2013).